Colloids and Surfaces B: Biointerfaces 102 (2013) 708–717

Contents lists available at SciVerse ScienceDirect

Colloids and Surfaces B: Biointerfaces

journal homepage: www.elsevier.com/locate/colsurfb

An investigation on the cytotoxicity and caspase-mediated apoptotic effect of biologically synthesized silver nanoparticles using *Podophyllum hexandrum* on human cervical carcinoma cells

Murugaraj Jeyaraj[a], Manoharan Rajesh[a], Renganathan Arun[b], Davoodbasha MubarakAli[c], Gnanasekar Sathishkumar[a], Ganeshan Sivanandhan[a], Gnanajothi Kapil Dev[a], Markandan Manickavasagam[a], Kumpati Premkumar[b], Nooruddin Thajuddin[c], Andy Ganapathi[a,*]

[a] *Department of Biotechnology and Genetic Engineering, School of Biotechnology, Bharathidasan University, Tamil Nadu, India*
[b] *Cancer Genetics and Nano-medicine Laboratory, Department of Biomedical Sciences, Bharathidasan University, Tamil Nadu, India*
[c] *Department of Microbiology, Bharathidasan University, Tamil Nadu, India*

ARTICLE INFO

Article history:
Received 24 August 2012
Received in revised form
26 September 2012
Accepted 27 September 2012
Available online xxx

Keywords:
Silver nanoparticles
Podophyllum hexandrum
Cytotoxicity
DNA damage
HeLa cells

ABSTRACT

Now-a-days synthesis and characterization of silver nanoparticles (AgNPs) through biological entity is quite interesting to employ AgNPs for various biomedical applications in general and treatment of cancer in particular. This paper presents the green synthesis of AgNPs using leaf extract of *Podophyllum hexandrum* Royle and optimized with various parameters such as pH, temperature, reaction time, volume of extract and metal ion concentration for synthesis of AgNPs. TEM, XRD and FTIR were adopted for characterization. The synthesized nanoparticles were found to be spherical shaped with average size of 14 nm. Effects of AgNPs were analyzed against human cervical carcinoma cells by MTT Assay, quantification of ROS, RT-PCR and western blotting techniques. The overall result indicates that AgNPs can selectively inhibit the cellular mechanism of HeLa by DNA damage and caspase mediated cell death. This biological procedure for synthesis of AgNPs and selective inhibition of cancerous cells gives an alternative avenue to treat human cancer effectively.

1. Introduction

Cancer is one of most important scourges of mankind and responsible for major mortality, more than ten million people are diagnosed with the disease annually, it was developed through various cellular physiological systems such as cell signaling and apoptosis. With the prevalence and the emergence of multiple drug resistance, nonspecific systemic distribution of antitumor agents, inadequate drug concentrations reaching the tumor site, intolerable cytotoxicity and limited ability to monitor therapeutic responses because of these challenges cancer became incurable. To overcome this problem it is necessary to develop and design new strategies, tools and drugs for the diagnosis and treatment of cancer [1].

With the advent of nanotechnology there are different types of nano sized materials have been developed for wide range applications in materials science to biological science in general and nanomedicine in particular. These particles have been significantly used in various fields including drug delivery, catalysis, environmental pollution control and material chemistry [2–5] and so on. Nanoparticles with the size range between 1 and 1000 nm are mainly explored for the diagnosis and treatment of human cancers which led to the new discipline of nano-oncology [6].

Among different nanoparticles exploited, silver nanoparticles (AgNPs) are one of the promising nanoproduct widely used in the field of nanomedicine because of their unique properties. AgNPs having pinnacle antimicrobial activity against Gram-positive and Gram-negative bacteria, fungi, protozoa and certain viruses [7]. Apart from this, recently the antitumor effect of AgNPs has been reported against different cancerous cell lines [8]. The main drawback of physical and chemical methods for nanoparticles synthesis is the utilization of hazardous chemicals and high energy. At present there has been a considerable interest in the biological synthesis of nanoparticles because of its simple, safe and eco-friendly principles [9]. Different types of biological entities such as plants, fungi, yeast, cyanobacteria and bacteria have been employed for the synthesis of nano scale particles. Compare to other microbial entities plants extract mediated synthesis of nanoparticles is more significant because it is less-expensive, does not require elaborate

* Corresponding author. Tel.: +91 431 94434 44957; fax: +91 431 2407045.
E-mail addresses: jeymuruga@gmail.com (M. Jeyaraj), aganapathi2007@gmail.com (A. Ganapathi).

0927-7765/$ – see front matter © 2012 Elsevier B.V. All rights reserved.
http://dx.doi.org/10.1016/j.colsurfb.2012.09.042

process such as microbial maintenance and multiple purification steps [10–12].

Podophyllum hexandrum Royle belongs to Beriberdaceae described as 'Aindri' – a divine drug in the traditional Indian system of medicine 'the Ayurveda' [13], and has also been used in the traditional Chinese system of medicine for treatment of a number of ailments. In modern allopathic system of medicine, this plant has been used for the treatment of various metabolic disorders, venereal warts and infections [14,15]. The abundant presence of polyphenols, lignans and nitrate reductase was reported in *P. hexandrum* and their role in the bio-reduction of AgNPs has also been suggested [16]. Therefore, the current interest is to synthesis AgNPs by employing the leaf extract of medicinal plant *P. hexandrum* as a novel reducing agent. Synthesized particles were characterized and evaluated for its anticancer potential against HeLa cell line under in vitro condition. Cytotoxicity and caspase-mediated apoptotic effects of synthesized AgNPs were monitored through different analysis such as MTT, COMET, DNA fragmentation, AO-EB, RT-PCR and Western blotting.

2. Materials and methods

2.1. Chemicals

Silver nitrate ($AgNO_3$), cisplatin, Hoechst 33258, 3-(4,5-dimethyl-2-thiazolyl)-2,5-diphenyl-2H-tetrazolium bromide (MTT), 2-7-diacetyl dichlorofluorescein (DCFH-DH), heat inactivated fetal calf serum (FBS), minimum essential medium (MEM), glutamine, EDTA and trypsin were purchased from Sigma–Aldrich (St. Louis, USA).

2.2. Cell culture

Human cervical cancer cells (HeLa) were obtained from National Centre for Cell Science (NCCS), India. These cell lines were grown as a monolayer in MEM, which was supplemented with 10% FBS, 1% glutamine, 100 IU/ml of penicillin and 100 μg/ml of streptomycin and incubated at 37 °C in 5% CO_2 with 95% humidity. The HeLa cells were maintained in 75 cm^2 tissue culture flask.

2.3. Biosynthesis of silver nanoparticles

Fresh leaves (5 g) of *P. hexandrum* were surface cleaned with running tap water, followed by distilled water, chopped into small pieces and boiled with 100 ml of Milli-Q water for 5 min. This extract was filtered through sterile muslin cloth followed by Whatmann No.1 filter paper and this filtrate was used for further experiments. For the synthesis of AgNPs different parameters such as temperature (20 °C, 30 °C, 40 °C, 50 °C and 60 °C), pH (4.5, 6.0, 7.5, 9.0 and 10), time (30, 60, 90, 120 and 150 min), concentration of metal ion(0.25 mM, 0.5 mM, 1 mM, 1.5 mM, 2 mM, 3 mM) and volume of leaf extract (*PHLE*) (1.5, 3, 5, 7.5, and 10 ml) were optimized. The reaction mixture was periodically monitored using UV–vis spectrophotometer in the ranges of 300–600 nm.

2.4. Purification of AgNPs

Purification of AgNPs was done with sucrose gradient centrifugation that already described earlier [17]. For that, the particles were washed five times by centrifugation and re-dispersed in water to remove excess of silver. They were then transferred to a dialysis tube with a 12,000 Da molecular weight cutoff. Nanoparticles were re-suspended in 1 ml of HEPES buffer (20 mM; pH 7.4) supplemented with sucrose to reach a density of 2.5 g/ml and a gradient was made. The solution was placed at the bottom of a centrifuge tube (13 ml). Twelve milliliters of a linear gradient of sucrose (0.25–1 M) density was layered on the nanoparticles suspension and subjected to ultracentrifugation (200,000 × *g* at 4 °C for 16 h) by using an SW41 rotor (Beckman Instruments, Fullerton, CA, USA).

2.5. High-throughput characterization of AgNPs

Biosynthesized nanoparticles have been quantified by measuring the absorbance of mixtures using UV–vis spectrophotometer (JASCO V-650, Japan) in the ranges of 300–600 nm. Synthesized AgNPs were centrifuged and lyophilized to make them into powder. The freeze dried powder was subjected to FTIR analysis adopting with conditions of 400–4000 cm^{-1} with a resolution of 4 cm^{-1} in KBr pellets. X-ray diffraction was performed for determination of the dimension of biologically synthesized AgNPs with *h*, *k*, *l* values. The diffraction pattern was obtained with conditions at 40 kV and 30 mA in *Cu*, *Ka* radiation and particles size (*L*) using (PAN analytical X pert PRO Model) of the silver was calculated using following Debye–Scherrrer's equation.

$$L = \frac{0.9\lambda}{\beta \cosh \theta} \quad (1)$$

where, λ is the wavelength of the X-ray, β is full width and half maximum and θ is the Bragg's angle. Finally, a drop of synthesized nanoparticles placed on the carbon coated grid and allowed to dry. Size and shape of the nanoparticles were observed by adopting transmission electron microscopy (TEM) (TECNAI-10) operated at an accelerating voltage of 100 kV.

2.6. Experimental evidences on anti-cancerous activity of AgNPs

Effects of AgNPs on cancer cell line was determined through different experiments, such as MTT, ROS quantification, Apoptotic effect of AgNPs on HeLa was confirmed with AO/EB and Hoechst staining. DNA damage of AgNPs treated cells was determined by COMET and DNA fragmentation assays. Protein expression pattern and caspase mediated apoptotic effects will be further screened with RT-PCR and Western blotting analysis.

2.6.1. Cytotoxicity of AgNPs on HeLa cells – MTT assay

The MTT assay is a colorimetric, non-radioactive assay for measuring cell viability through increased metabolization of tetrazolium salt [18]. HeLa cells in the concentration of 1×10^6 cells/ml were taken into 96 well plates. Then, the cells were treated with different concentration of AgNPs (0–50 μg/ml) and incubated in the presence of 5% CO_2 and 95% humidity at 37 °C for 24 h. MTT (5 mg/ml) was added to the incubated-cells, then further incubated for another 4 h. The crystals were dissolved in 200 μl of DMSO and the absorbance was measured in a colorimetric at 570 nm with reference filter as 655 nm.

2.6.2. Quantification of intracellular ROS

The intracellular ROS levels were measured by 2′,7′-dichlorodihydrofluorescein (DCFH-DA) method [19]. For that, experimental cells were incubated with 10 μM DCFHDA for 30 min at 37 °C in the dark, washed twice with PBS and the cells were observed under a Nikon TCF100 fluorescent microscope.

2.6.3. Apoptotic assays

Acridine orange/ethidium bromide (AO/EB) staining was carried out to detect morphological evidence of apoptosis on the AgNPs treated cells [20]. The cells were fixed in 3:1 ratio of methanol and glacial acetic acid for 1 h at room temperature. The cells were labeled with 1:1 ratio of AO and EB in PBS and incubated for 5 min then the excess unbinding dye was removed by

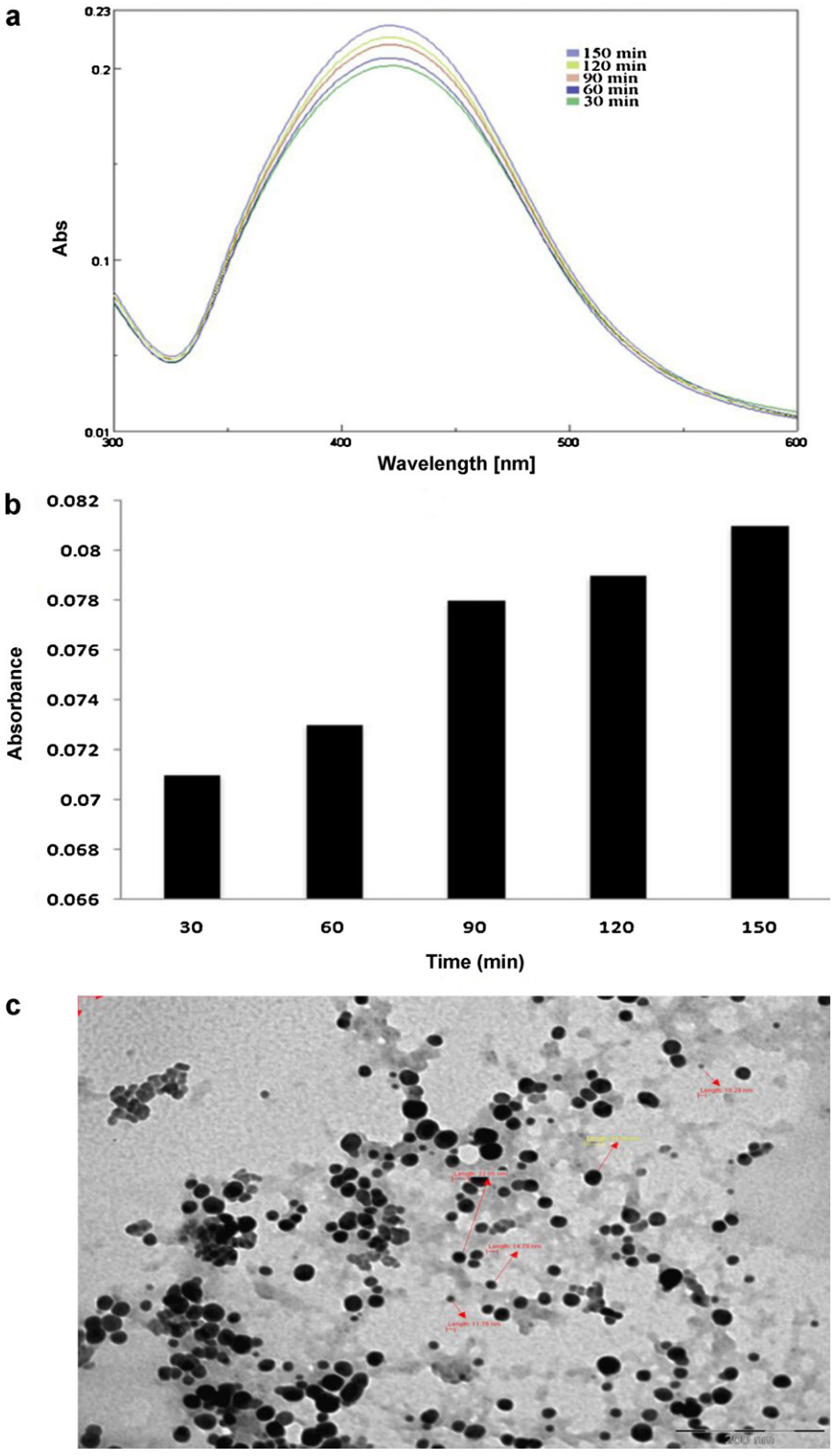

Fig. 1. (a) UV–vis spectra of synthesized AgNPs at different time intervals, (b) histogram represents the variation in the absorbance spectra, (c) TEM micrograph of synthesized AgNPs.

washing with PBS. Stained cells were visualized under UV illumination using the 40× objective (Nikon 80i Eclipse, Japan) and the digitized images were captured. The apoptotic cells with the shrunken, fragmented nuclei and brightly fluorescent and necrotic cells as ethidium bromide positive were scored and the percentage of apoptotic cells was calculated. Furthermore, AgNPs-induced apoptosis in HeLa cells was assessed by Hoechst 33258 staining. Treated with 20 μg/ml AgNPs for 24 h, the cells were harvested and smeared on slides. The slides were air-dried, fixed in methanol-acetone (3:1 v/v), and stained with Hoechst 33258 (5 μg/ml) at

37 °C for 20 min. Nuclear morphology was examined under fluorescence microscopy (Nikon 80i Eclipse, Japan) to identify cells undergoing apoptosis.

2.6.4. COMET and DNA fragmentation assays for DNA damage

DNA damage was estimated by alkaline single cell gel electrophoresis (COMET assay) [21]. A layer of 1% NMPA (normal-melting-point-agarose) was prepared on microscopic slides along with the HeLa cells were mixed with 0.5% LMPA (low-melting-point-agarose). The suspension was pipette onto the pre-coated slides. It was immersed in cold lysis solution at pH 10.0 (2.5 M NaCl, 100 mM Na_2-EDTA, 10 mM Tris pH 10, 1% Triton X-100, 10% DMSO) and kept at 4 °C for 60 min. The slides were then placed in alkaline electrophoresis buffer at pH 13 and left for 25 min. Subsequently, the slides were transferred to an electrophoresis tank with fresh alkaline electrophoresis buffer and electrophoresis was performed at electric field strength of 1.33 V/cm for 25 min at 4 °C. The slides were neutralized in 0.4 M Tris (pH 7.5) for 5 min and stained with ethidium bromide (25 μl in 50 μg/ml). For visualization of DNA damage, observations were made using a 40× objective in an epifluorescent microscope equipped with an excitation filter of 510–560 nm and a barrier filter of 590 nm. DNA damage was quantified by tail moment, tail length, olive tail moment (OTM). In addition, DNA fragmentation assay also adopted for the same, in which cells were collected after 24 h of the treatment with AgNPs and cisplatin (30 μg/ml) as a standard positive control. DNA fragments were isolated according to the standard protocol for DNA isolation [22]. Briefly, after the treatment for 24 h, cells were harvested, counted and washed with 1X PBS at 4 °C. The cells were pelleted by centrifugation at 200 × *g* at 4 °C. The pellet was suspended in DNA lysis buffer [1 M Tris (pH 8.0), 0.5 EDTA and 75% sodium lauryl sarcosine] and incubated overnight with proteinase K (0.5 mg/ml) at 50 °C. After overnight incubation, RNase (50 μg/ml) was added and again incubated for 1 h at 50 °C. DNA was extracted using phenol: chloroform (1:1 v/v) and then, electrophoresed in 2% agarose gel for 2 h at 50 V. The gel was stained with ethidium bromide (0.5 μg/ml) and photographed in Gel Doc™ XR+ (Bio-Rad, CA, USA).

2.6.5. Semi-quantitative RT-PCR analysis

Total RNA was extracted from experimental cells using Trizol reagent (Invitrogen, USA). RNA isolated from cells was reverse-transcribed and amplified using the one-step RT-PCR System (Fermentas, USA). Primer sequences of forward and reverse Bax (NM_001188.3) were 5′-GCC ACCAGC CTG TTT GAG-3′ and 5′-CTG CCA CCC AGC CAC CC-3′, for Bcl2 (NM_000657.2) it was 5′-TATAAG CTG TCG CAG AGG GGC TA-3′ and 5′-GTA CTC AGT CAT CCA CAG GGCGAT-3′ and for GAPDH (NM_002046.3) it was 5′-AAT CCC ATC ACC ATC TTC CA-3′ and 5′-CCT GCTTCA CCA CCT TCT TG-3′, respectively. PCR conditions as follows: 94 °C for 5 min; 35 cycles of 94 °C for 1 min, 55–62 °C for 1 min, 72 °C for 1 min; and final extension step of 72 °C for 10 min. The products were verified by agarose gel electrophoresis as well. The level of GAPDH gene expression served as an internal control.

2.6.6. Western blotting

HeLa cells were cultured in 6-well plates and then treated with or without AgNPs and cisplatin for 24 h. The cells were then lysed in the buffer containing 50 mM Tris–Cl (pH 8.0), 150 mM NaCl, 0.02% sodium azide, phenyl-methane sulfonyl fluoride (PMSF), aprotinin, and 1% Triton X100, and centrifuged at 12,000 × *g* for 30 min at 4 °C. Quantified proteins were performed in SDS-PAGE. The separated proteins were transferred to nitrocellulose membranes. Membranes were washed with Tris-buffered saline Tween-20 (TBST), blocked with 5% skimmed milk for 1 h at 37 °C, incubated overnight at 4 °C with either goat anti-rabbit caspase 3, 8 and 9 or β-actin antibodies at the manufacturer recommended dilutions. After incubation, the membrane is washed with TBST buffer. The membranes were then incubated with secondary mouse anti-goat peroxidase conjugated antibodies (Cell Signaling Technologies, USA) for 1 h at 37 °C. After washing membranes with TBST, they were developed with DAB chromogenic detection method and scanned.

3. Results

3.1. Biosynthesis of nanoparticles

When the leaf extract was mixed with $AgNO_3$, the biosynthesis reaction started within few minutes. Clear $AgNO_3$ solution was changed into brown color due to the excitation of surface plasmon resonance indicates the formation of AgNPs. The peak area at 420 nm increased with increase in reaction time at all concentrations revealed the maximum production of AgNPs. Effective synthesis of AgNPs was observed in lower pH compare to alkaline pH, increasing the temperature (20 °C–60 °C) shows variation in the yield of AgNPs. Synthesis was found higher at 60 °C when compared to below 60 °C. Synthesis of AgNPs has direct proportion with time and *PHLE* quantity, it shows maximum absorbance at 420 nm. Increased absorbance spectra were noticed (1 mM $AgNO_3$) metal ion concentration indicates enormous yield of AgNPs. From this the overall optimized condition for the efficient synthesis of *PHLE* mediated AgNPs was resolved to be stoichiometric proportion of 10 ml *PHLE* in 1 mM $AgNO_3$, pH-4.5, temperature at 60 °C for 150 min to attain high yield of mono dispersed AgNPs. The optimized reaction condition synthesis AgNPs efficiently, which shows the increased SPR at 420 nm in different time intervals (Fig. 1a and b).

3.2. Characterization of nanoparticles

FTIR spectra of AgNPs synthesized by *P. hexandrum* shows the absorbance peaks at 1236 cm^{-1}–1384 cm^{-1} correspond to the amide III and II group, respectively. Peaks at 3431to 3776 cm^{-1} indicate polyphenolic group along with 617 cm^{-1} aromatic C—H vibrations. Further, peaks at 1028 cm^{-1}–1236 cm^{-1} indicate C—O single bond peaks at 1640 cm^{-1} represent carbonyl groups (C═O) from polyphenols and alkanes (2924 cm^{-1}) (Fig. 2). XRD patterns of the AgNPs showed two prominent Bragg reflections which were indexed on the basis of fcc structure of silver. The intensities of (1 1 1) and (2 0 0) diffraction peaks were corresponding to 38.13° and 43.92°, respectively and confirmed the crystalline nature of the biosynthesized AgNPs (Fig. 3). It is suggested that all the particles are of acceptable crystallinity with cubic structure. It is also noticed that the diffraction angles of AgNPs are quite close to bulk silver crystal ($2\theta = 38.12°$). The particle size (L) was calculated as 10 nm and it was also confirmed by TEM, which shows the particles are predominantly in spherical shape with a diameter ranging between 12 and 40 nm (Fig. 1c). No definite agglomeration of nanoparticles was noticed, which represents the polydispersity of nanoparticles. Most of the particles were spherical in shape with smooth edges and some nanoparticles were observed as irregular circles without uniform edges.

3.3. In vitro anti-cancerous activity of synthesized AgNPs

3.3.1. Effect of AgNPs induced cytotoxicity on HeLa cells

The cytotoxicity on HeLa cell lines were increased with increased concentration of AgNPs. There was a change in the percentage of cell viability in control and AgNPs (0, 5, 10, 20, 30, 40, and 50 μg/ml) treated HeLa cells (Fig. 4). Complete mortality rate that is 100% cell death was observed in 50 μg/ml concentration of AgNPs. Hence, the inhibitory concentration at 50% (IC_{50}) was fixed at 20 μg/ml of AgNPs for HeLa cells. Further experiments have been

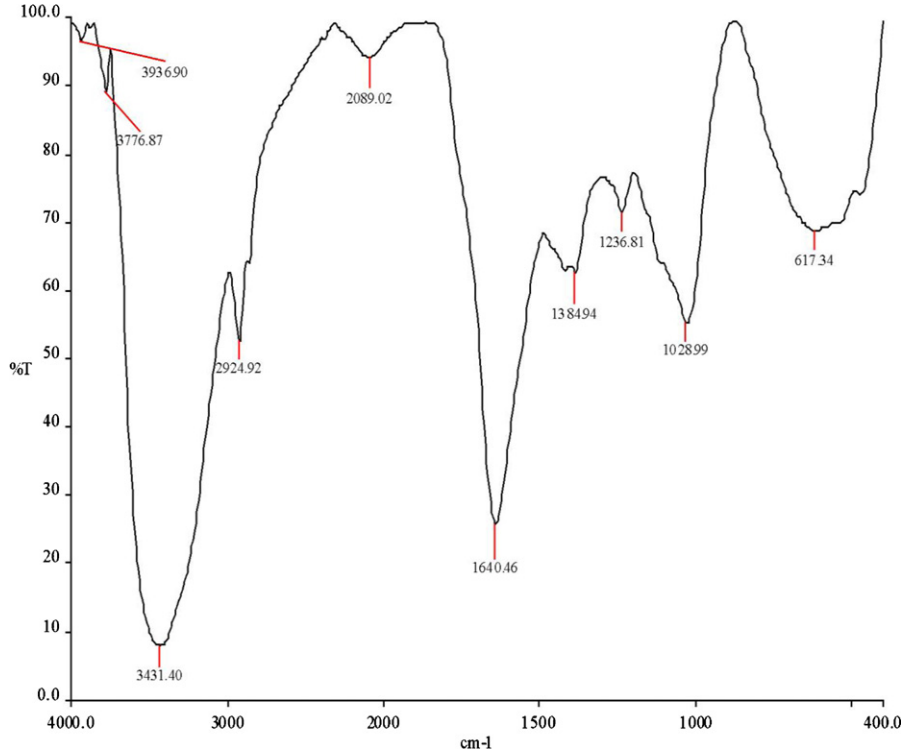

Fig. 2. FTIR-spectrum of AgNPs showing functional group of the plant extract reacted with silver nanoparticles.

carried out with 20 μg/ml for AgNPs and the standard anticancer drug cisplatin (30 μg/ml) was also used in this study to confirm and correlate the anticancer activity of AgNPs.

3.3.2. Measurement of ROS levels in AgNPs pretreated cells

The DCFH-DA method measures intracellular generation of hydrogen peroxide, an indirect procedure for estimating ROS. In the present study the intracellular ROS concentration was significantly higher in AgNPs treated HeLa cells when compared to the cisplatin (30 μg/ml) treated groups. It was measured to investigate the potential role of oxidative stress as a mechanism of AgNPs induced toxicity. It is now well established that the generation or external addition of ROS can cause cell death by two distinct pathways, viz. apoptosis or necrosis (Fig. 5).

3.3.3. AgNPs induces apoptosis in HeLa cells

An attempt was made to verify whether the inhibitory action of the AgNPs on the *HeLa* cells was due to the apoptosis. The apoptosis was noticed with the morphological changes in the cell shape and chromatin condensation, these morphological changes are due to the activation of caspase cascades, which cleaves the specific substrates responsible for the DNA repair activation. The ability of the AgNPs to induce apoptosis was determined by acridine orange and ethidium bromide staining. After treatment with mentioned concentration, the cell were harvested and stained with acridine orange/ethidium bromide as mentioned in the materials and methods section. The stained cells were characterized to viable (light green), early apoptotic (bright green fluorescence and condensed

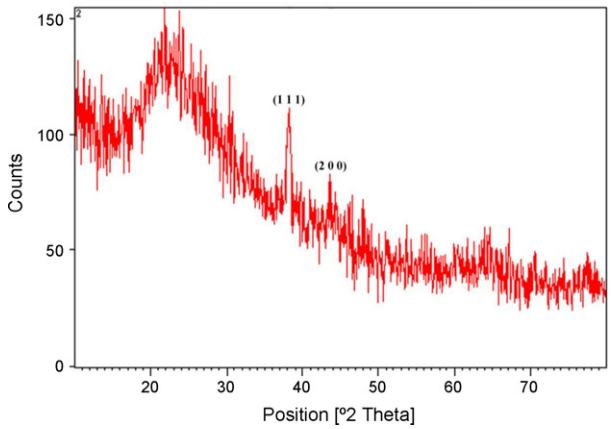

Fig. 3. XRD pattern of the silver nanoparticles index at (1 1 1) and (2 0 0) corresponds to spherical shaped nanoparticles.

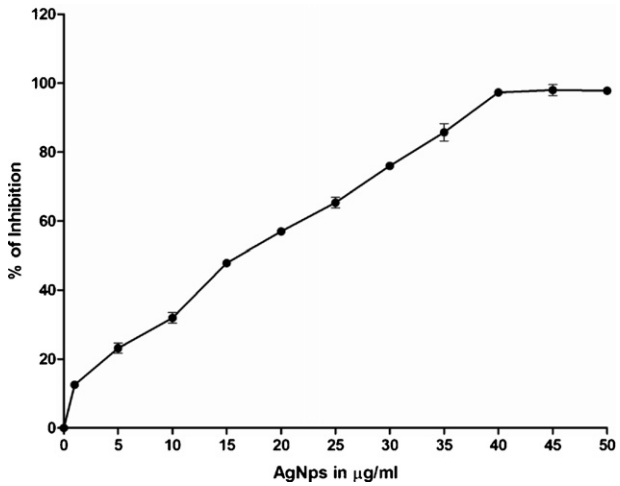

Fig. 4. Cytotoxicity of AgNPs on HeLa cells: increased concentration of AgNPs (0–50 μg/ml) (*X*-axis) inhibits the growth of cells up to 100% (*Y*-axis) all the data were expressed in mean ± SD of three experiments.

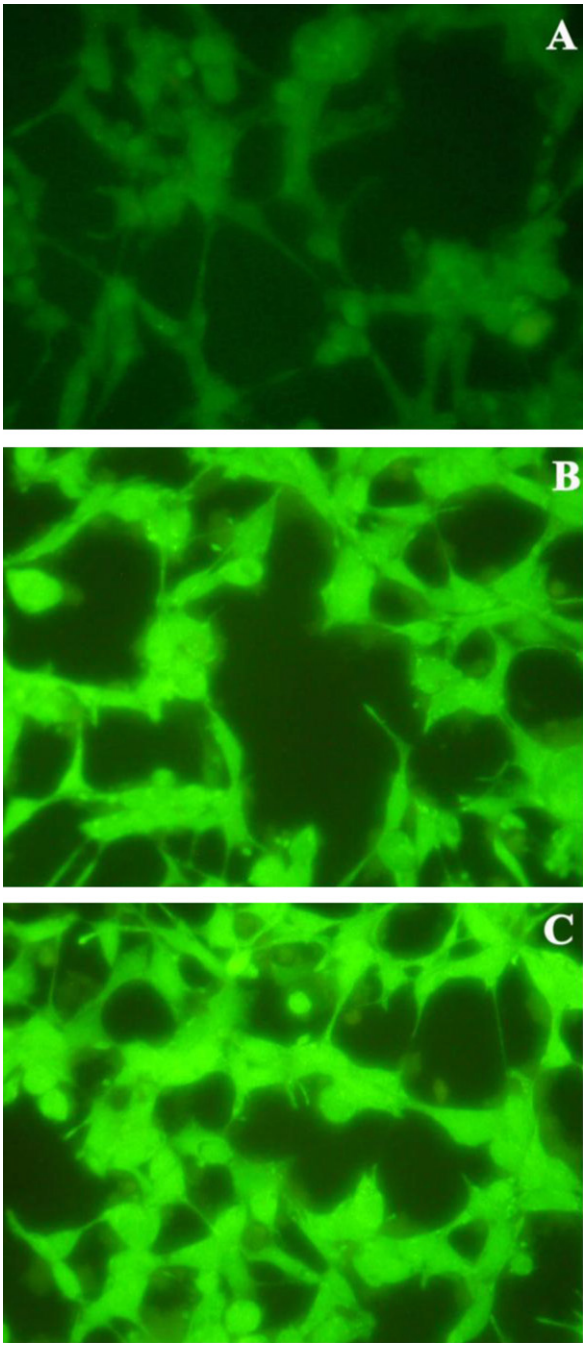

Fig. 5. Effect of AgNPs on ROS generation in HeLa cells. (A) Control, (B) positive control (cisplatin) and (C) AgNPs (20 μg/ml).

chromatin), late apoptotic cells (orange fluorescence) and non-viable cells (red colored fluorescence) (Fig. 6a). AgNPs treated cells condensed nuclei, membrane blebbing and apoptotic bodies, in contrast the control cells showed intact nuclear architecture. Compare to the positive control cisplatin AgNPs shows much greater apoptotic effect (Fig. 6c). Furthermore, the effects of AgNPs on *HeLa* cells gross nuclear morphology were observed under fluorescence microscopy after Hoechst 33258 staining. After the treatment with 20 μg/ml AgNPs for 24 h, HeLa cells began to exhibit apoptotic characteristics such as cell shrinkage, nuclear condensation, and fragmentation. In the control group, the cells were regular in morphology and grew fully in patches and were confluent, rarely sloughing off (Fig. 6b).

3.3.4. Effect of AgNPs induced DNA damage on HeLa cells

AgNPs induces the apoptosis in treated HeLa cells through DNA damage that will be noticed in comet and DNA fragmentation assays. The induction of DNA single strand break is often used to predict oxidative damage of tumor cells. As in (Fig. 7a), the AgNPs pre-treatment changes the levels of DNA damage (number of DNA in tail, tail length, tail moment and olive tail moment) in HeLa cells and there is no change in untreated control was observed. Furthermore, we also observed tail DNA in AgNPs treated cells which appeared during single cell gel electrophoresis. AgNPs treatment significantly increased number of tail DNA, tail length, tail moment, olive tail moment in HeLa cells. The presence of oligonucleosomal DNA damage at AgNPs concentration around 20 μg/ml indicates apoptotic cell death. AgNPs induced DNA damage was further confirmed by DNA laddering assay (Fig. 7b) which shows that the DNA ladder was formed in the AgNPs treated cells. Collectively, these data confirms that AgNPs has induced the cell death through apoptotic pathway.

3.3.5. AgNPs induce apoptosis via a mitochondria- and caspase-dependent pathway

It was explored that the possible molecular mechanisms of AgNPs-mediated cell death, the apoptotic regulators have been measured through mRNA and protein expression patterns. In order to confirm the AgNPs induced ROS is activate the apoptotic pathway mRNA levels of Bcl-2 and Bax were semi-quantitatively determined through RT-PCR. All the expression was normalized with the levels of the b-actin expression (Fig. 8a). The mRNA expressions of the above genes after the AgNPs treatment were also compared with positive control as cisplatin. Similarly, triggering the apoptosis was identified through the activation of the caspase cascades. In this study the activation of caspases (3, 8 and 9) were detected through immunoblotting and binding with specific antibodies (Fig. 8b).

4. Discussion

Biological synthesis of AgNPs was achieved using the plant, *P. hexandrum* leaf extract, the color change was observed after the addition of *PHLE* to $AgNO_3$ solution due to the excitation of Surface Plasmon Resonance confirms the generation of AgNPs. In UV–vis spectrometer, the absorbance spectra was observed at 420 nm, this shift has been suggested due to the availability of more reducing biomolecules for the reduction of silver ions at higher concentration. The change in absorbance has direct correlation with the concentration and may be due to the presence of reducing agents such as nitrate reductase, polyols like terpenoids, flavonoids and polysaccharides [23]. Apart from this plant proteins are reported to bind with nanoparticles either through free amine groups or cysteine residues [24–26].

These results clearly indicates that AgNPs synthesized with *P. hexandrum* leaf extract were surrounded by some metabolites like terpenoids that have functional groups of amines, alcohols, ketones, aldehydes, and carboxylic acids. Terpenoids are reported to be surface active molecules for nanoparticles synthesis in *Azadirachta indica* leaf [27]. The mechanism by which nanoparticles formed in biosynthesis procedures is not clear. Reduction of silver ions is necessary for nanoparticles generation, it was noticed that the cyclic peptide curcacycline A&B present in the latex of *Jatropha curcus* plays a crucial role for the reduction of Ag^+ to Ag^0 and also act as a stabilizing agent [28].

Biomaterial dosage is an important criterion in crystallization of AgNPs as they are the source of reductant that determines the biosynthesis of nanoparticles. Variation in initial concentration of *P. hexandrum* leaf extract did not affect the shape and size of the nanoparticles formed. A vast difference in size and shape of the

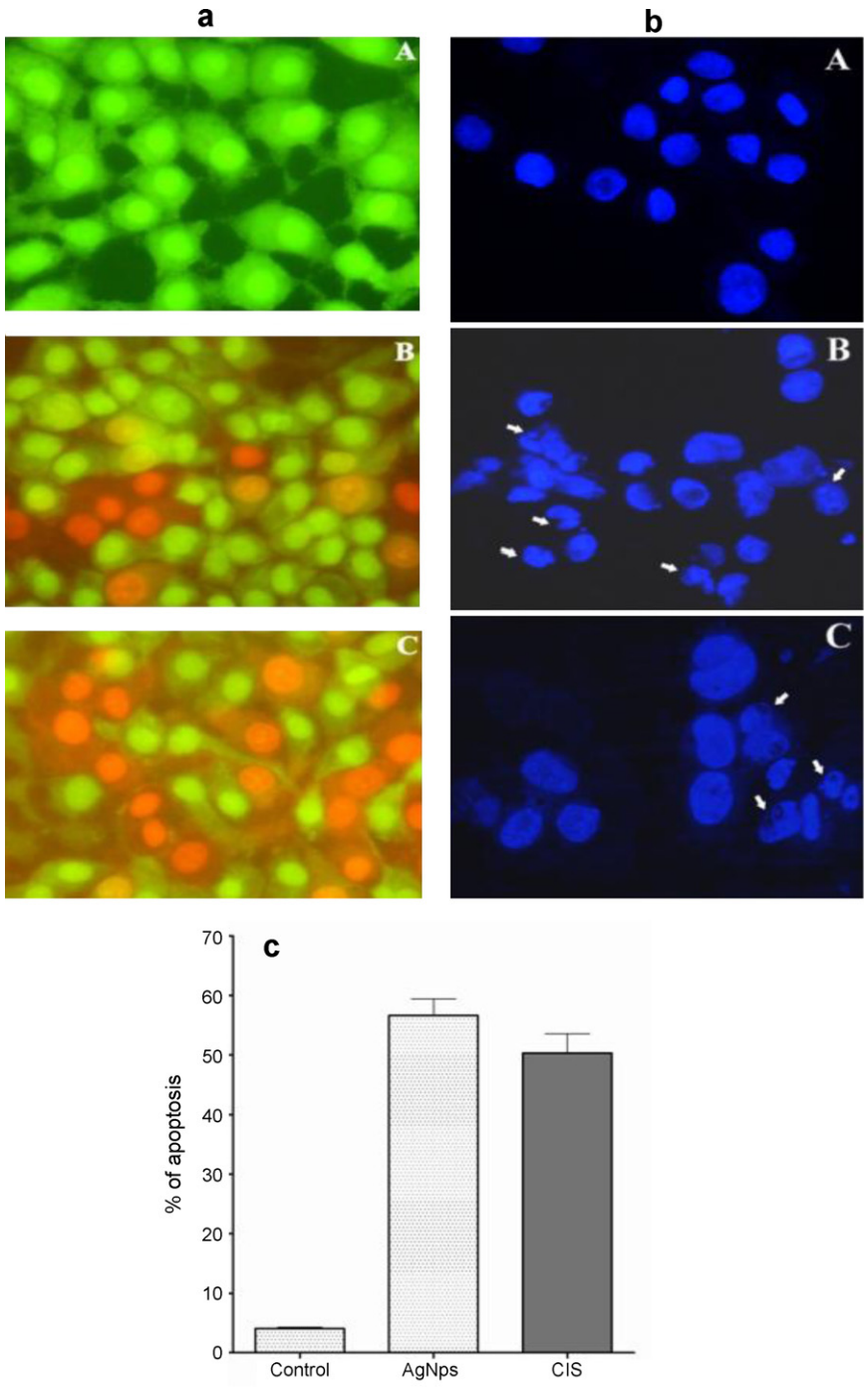

Fig. 6. Effect of AgNPs on apoptotic morphological changes in HeLa cells (a) AO/EB staining, (b) Hoechst 33258 and (c) total percentage of apoptosis. All the data were expressed in mean ± SD of three experiments. (A) Control, (B) positive control (cisplatin) and (C) AgNPs (20 μg/ml).

AgNPs has been reported in *Cinnamomum camphora* leaf powder [23]. In this present study, the density of particles was found to be proportional to increasing *P. hexandrum* leaf extract concentration, which can be attributed to the higher concentration of reductive material. In general synthesis of AgNPs direct proportion with the quantity of reducing agent, high dosage of reducing agent will give maximum yield [23,29]. It has been reported that there was an increase in absorbance values with increasing fruit extract's quantities of *Tanacetum vulgare* [30]. Variation in the pH before and after the synthesis of AgNPs was observed, after synthesis pH of the colloid is lower in most cases. In alkaline pH, the aggregation of AgNPs was believed to be favored over the nucleation to form new and large sized nanoparticles. Our result highly correlates with result of [31], their report confirms the vital role of pH in controlling the shape and size of the AgNPs. It was believed that reduced synthesis of nanoparticles was obtained at low temperature because at lower temperature the Plasmon band was not accompanied with increased intensity. [32]. Increase in temperature reflects in the intensity of SPR peak due to increasing rate of nanoparticles synthesis [33] showed the sharpness of the absorbance peak depend on size of the nanoparticles.

The present study demonstrated that higher metal ion concentration played a vital role in synthesis of AgNPs, while the particle synthesis rate was negligible at lower concentration. This result

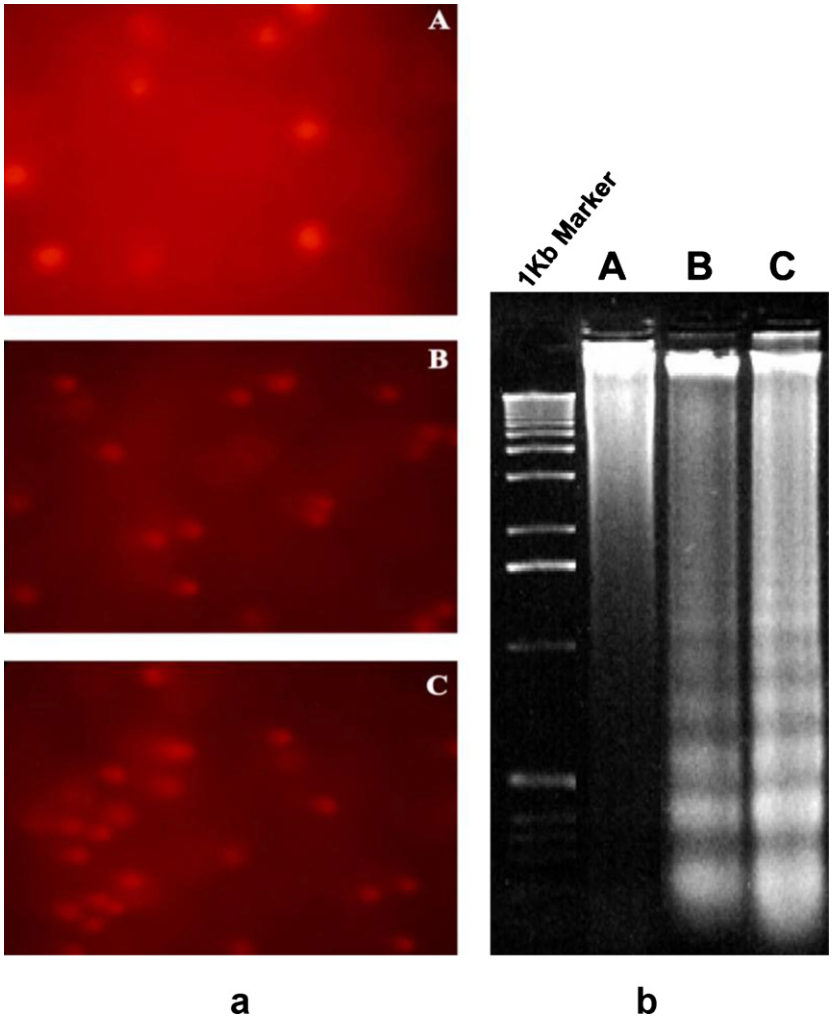

Fig. 7. Effect of AgNPs on DNA damage in HeLa cells by (a) comet assay and (b) DNA fragmentation assay. (A) Control, (B) positive control (cisplatin) and (C) AgNPs (20 μg/ml).

corroborate with the results of [34] where the peak absorbance and size of the nanoparticles were enhanced with increasing the metal ion concentrations from 0.1 to 5 mM. Yield of AgNPs was direct proportion with reaction time also reported that the peak absorbance was sharper when the contact time was increased at 2 h time duration. We observed that AgNPs treatment (24 h of incubation) have significantly decreased the percentage of cell viability in HeLa cells. This result is comparable to the one reported by [35] where cytotoxicity due to decreased mitochondrial function was indicated in a rat liver derived cell line (BRL 3A) that was exposed to AgNPs at concentrations in the range of 5–50 μg/ml. Previous reports showed that AgNPs can induce oxidative cell damage in human liver cells through inhibition of mitochondria-involved apoptosis [36].

In this study, we evaluated the anticancer activity of AgNPs in human cervical cancer cell line in vitro, decreased mitochondrial in cells exposed to AgNPs (0–50 μg/ml) in a dose-dependent manner as seen in the MTT assay. ROS are known to trigger the apoptotic cascade, via caspases, which are considered as the executioners of apoptosis [37]. Many studies have implicated that intracellular ROS in the signal transduction pathways leading to apoptosis [38,39]. Recently, it was reported that apoptosis induced by exposure to AgNPs was mediated by oxidative stress in fibroblast, muscle and colon cells [40]. In the present study, a fluorogenic assay was used to measure the production of ROS at 24 h culture setup, interestingly we observed significant increases in ROS generation during AgNPs (20 μg/ml) treatment. These data suggest that AgNPs and Ag^+ can induce cell death in HeLa cells through a ROS-mediated apoptotic process as suggested in the prooxidant effect in HeLa cells. The increased ROS levels and subsequent loss of mitochondria membrane potential might be the reason for the increased apoptotic morphological changes in the AgNPs treated cells. However, late apoptotic cells can be falsely detected as necrotic cells due to membrane damage. Accordingly, cells testing positive of apoptosis at an early time point could be detected as necrotic cells after longer exposures [41]. Apoptosis has previously been found to occur in response to treatment with other nanomaterials such as TiO_2 [42], NP realgar powders [43] and nanoscale hydroxyapatite [44]. At higher doses of AgNPs, however, necrotic changes are seen. Previous reports showed that the AgNPs were found to increase the DNA tail length in a comet assay, which measures DNA strand breaks as well as alkali labile sites [45].

It was observed that there was increase in internucleosomal DNA fragmentation due to activation of intracellular caspase enzyme and oxidative stress in cell in the present study. It has been reported that the ZnO and ZnPc nanoparticles, which stimulate the apoptotic signaling pathway and facilitate the DNA fragmentation that implies that biochemical hallmark of apoptosis and graphene nanoparticles also induces the oxidative stress in mitochondria and apoptotic DNA fragmentation [46,47]. Therefore, in the present study we have highlighted the correlations among cytotoxicity, oxidative stress and apoptotic potential of AgNPs. Since AgNPs are used in an increasing number of applications, further studies on

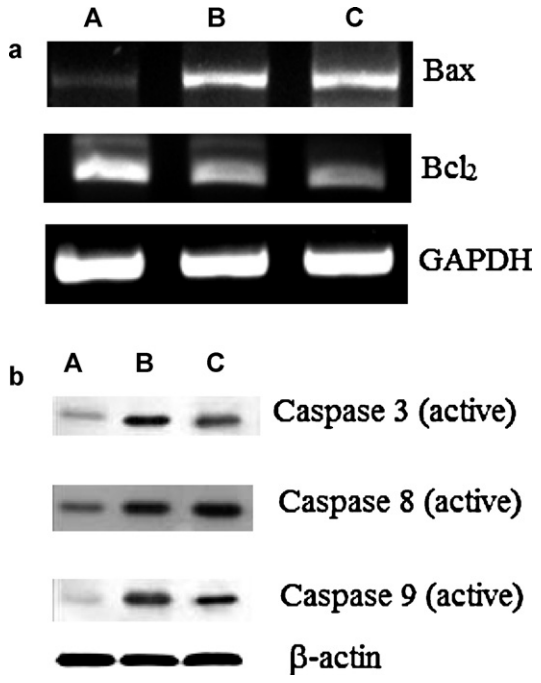

Fig. 8. (a) Effect of AgNPs on mRNA levels of Bcl2 and Bax in HeLa cells. (A) Control, (B) positive control (cisplatin) and (C) AgNPs (20 μg/ml). (b) Effect of AgNPs on caspase 3, 8 and 9 protein expression as determined by Western blot analysis in HeLa cell line. (A) Control, (B) positive control (cisplatin) and (C) AgNPs (20 μg/ml) β-actin was used as the control. Representative Western blots of experiments performed in triplicates.

the mechanisms of AgNPs uptake and cytotoxicity are required to assess the risks and benefits of nano-silver. Various studies have been reported that the AgNPs initiated the apoptosis through ROS generation in in vitro models [41]. However, the function of ROS in AgNPs induced HeLa cell growth inhibition is still lagging. Cervical cancer has been associated with disturbances in apoptotic regulation [48].

The apoptotic regulation is mainly depends upon the interbalance between Bcl-2 and Bax activity and also the other genes of their family for example Bad, Bcl-XL, Bcl-Xs and BAG1 [49,50]. In this study HeLa cells treated with AgNPs or cisplatin exhibited reduced levels of Bcl-2 expression, while Bax was increased. These results suggested that the mitochondrial pathway might be involved in AgNPs induced HeLa cell death. Mitochondria are important signaling centers during apoptosis, and the loss of mitochondrial integrity can be induced or inhibited by many regulators of apoptosis [51,52]. In many cases, oxidative stress induces caspase activation through cytochrome C releases from the mitochondrial inter-membrane space into the cytosol [53]. We showed in this study that AgNPs down-regulates the Bcl-2 as like cisplatin and up-regulated of Bax. This regulation of Bcl-2 and Bax initiates a cascade that lead to the activation of caspases (3, 8 and 9). Our results also demonstrated that AgNPs or cisplatin triggers the apoptosis by activating the caspase 3, 8 and 9. Thus, from this study mitochondria is may be a major site for AgNPs-induced ROS generation and which activates the intrinsic apoptotic pathway, which is characterized by modulation of Bax and Bcl-2 expressions in the mitochondria and thereby induces the cell death by caspase dependent pathway. These findings of green synthesized AgNPs from *P. hexandrum* may provide excellent avenue for health care and clinical therapeutic applications including cancer. Consequently, the cause underlying the cancer-specific cytotoxicity of green synthesized AgNPs was found to be the result of mitochondria-mediated cell death.

5. Conclusion

In summary, AgNPs have been successfully synthesized biologically using the leaf extract of *P. hexandrum* as a novel reducing agent, it was aimed to synthesis monodispersed nanoparticles by optimizing various parameters. Finally, anticancer property of synthesized AgNPs were screened against human cervical cancer cell line (HeLa), interestingly it was found that AgNPs initiates the cancer cell death by decreasing cell proliferation, increasing intracellular ROS, DNA damage and apoptosis. Synthesized AgNPs shows enhanced anticancer activity when compared with anti-cancer drug (cisplatin) depicts its potential anticancer value. The overall report emphasizes cost effective, single step and eco-friendly synthesis of AgNPs, flexibility of AgNPs could find applications in drug delivery and their application have been extended to cancer diagnosis and treatment.

Acknowledgements

All the authors are thankful to University Grant Commission (UGC) and Council for Scientific and Industrial Research (CSIR) for their grant by Rajiv Gandhi National Fellowship and Senior Research Fellowship.

References

[1] R.S. Acharya, S.K. Sahoo, Drug Discov. Today 15 (2010) 842–850.
[2] D.I. Gittins, D. Bethell, D.J. Schiffrin, R.J. Nichols, Nature 408 (2000) 67–69.
[3] C.R. Patra, R. Bhattacharya, D. Mukhopadhyay, P. Mukherjee, Adv. Drug. Deliv. Rev. 62 (2010) 346–361.
[4] T. Kiyonaga, T. Akita, H. Tada, Chem. Commun. (2011) 2011–2013.
[5] J. Robbens, C. Vanpars, I. Nobels, R. Blust, K.V. Hoecke, C. Janssen, Toxicology 269 (2009) 170–181.
[6] M.V. Yezhelyev, X. Gao, Y. Xing, A. Al-Hajj, S. Nie, R.M. O'Regan, Lancet Oncol. 7 (2006) 657–667.
[7] M.I. Sriram, S. Barath, M. Kanth, K. Kalishwaralal, S. Gurunathan, Int. J. Nanomed. 5 (2010) 753–762.
[8] P. Joshi, S. Chakraborti, J.E. Ramirez-Vick, Z.A. Ansari, V. Shanker, P. Chakrabarti, S.P. Singh, Colloids Surf. B: Biointerfaces 95 (2012) 195–200.
[9] D. MubarakAli, V. Gopinath, N. Rameshbabu, N. Thajuddin, Mater. Lett. 74 (2012) 8–11.
[10] D. MubarakAli, N. Thajuddin, K. Jeganathan, M. Gunasekaran, Colloids Surf. B: Biointerfaces 85 (2011) 360–365.
[11] V. Gopinath, D. MubarakAli, S. Priyadarshini, N. MeeraPriyadarshini, N. Thajuddin, P. Velusamy, Colloid and Surf B: Biointerfaces 96 (2012) 69–74.
[12] G. Sathishkumar, C. Gobinath, K. Karpagam, V. Hemamalini, K. Premkumar, S. Sivaramakrishnan, Colloids Surf. B: Biointerfaces 95 (2012) 235–240.
[13] G. Blasko, G.A. Cordell, H. Wagner, H. Hiroshi, N.R. Franworth, Plant Research, Academic Press, London, 1998.
[14] K.R. Beutner, G.V. Krogh, Semin. Dermatol. 9 (1990) 148–151.
[15] G. Gowdey, R.K. Lee, W.M. Carpenter, Endocrinology 79 (1999) 64–67.
[16] R. Chawla, R. Arora, R. Kumar, A. Sharma, J. Prasad, S. Singh, Mol. Cell. Biochem. 273 (2005) 193–208.
[17] S. Gurunathan, K.J. Lee, K. Kalishwaralal, S. Sheikpranbabu, R. Vaidyanathan, S.H. Eom, Biomaterials 30 (2009) 6341–6350.
[18] T. Moshmann, J. Immunol. Methods 65 (1983) 55–63.
[19] K. Hafer, K.S. Iwamoto, R.H. Schiestl, Radiat. Res. 169 (2008) 460–468.
[20] Z. Darzynkiewicz, X. Li, J. Gong, Methods Cell Biol. 41 (1994) 15–38.
[21] N.P. Singh, M.T. McCoy, E.L. Schneider, Exp. Cell. Res. 175 (1988) 184–191.
[22] R.T. Allen, W.J. Hunter, D.K. Agrawal, J. Pharmacol. Toxicol. Methods 37 (1997) 215–228.
[23] J. Huang, Q. Li, D. Sun, Y. Lu, Y. Su, X. Yang, Nanotechnology 18 (2007) 105104–105114.
[24] S.S. Shankar, A. Ahmad, M. Sastry, Biotechnol. Prog. 19 (2003) 1627–1631.
[25] A. Gole, C.V. Dash, V. Ramachandran, A.B. Mandale, S.R. Sainkar, M. Rao, Langmuir 17 (2001) 1674–1679.
[26] R. Vaidyanathan, S. Gopalram, K. Kalishwaralal, V. Deepak, S.R. Pandian, G. Sangiliyandi, Colloids Surf. B: Biointerfaces 75 (2010) 335–341.
[27] S.S. Shankar, A. Rai, A. Ahmad, M. Sastry, J. Colloid Interface Sci. 275 (2004) 496–502.
[28] H. Bar, D.Kr. Bhui, G.P. Sahoo, P. Sarkar, S.P. De, A. Misra, Colloids Surf. A: Physicochem. Eng. Asp. 339 (2009) 134–139.
[29] M. Sathishkumar, K. Sneha, Y.S. Yun, Bioresource Technol. 101 (2010) 7958–7965.
[30] S.P. Dubey, M. Lahtinen, M. Sillanpaa, Process Biochem. 80 (2010) 26–33.
[31] K. Sneha, M. Sathishkumar, S. Kim, Y.S. Yun, Process Biochem. 45 (2010) 1450–1458.
[32] D. Philip, Spectrochim. Acta Part A 73 (2009) 374–381.

[33] A.D. Dwivedi, K. Gopal, Colloids Surf A: Physicochem. Eng. Asp. 369 (2010) 27–33.
[34] S.M. Hussain, K.L. Hess, J.M. Gearhart, K.T. Geiss, J.J. Schlager, Toxicol. In Vitro 19 (2005) 975–983.
[35] M.J. Piao, K.A. Kang, I.K. Lee, H.S. Kim, S. Kim, Toxicol. Lett. 201 (2011) 92–100.
[36] B. Fadeel, A. Ahlin, J.I. Henter, S. Orrenius, M.B. Hampton, Blood 92 (1998) 4808–4818.
[37] M. Ott, V. Gogvadze, S. Orrenius, B. Zhivotovsky, Apoptosis 12 (2007) 913–922.
[38] S. Ueda, H. Masutani, H. Nakamura, T. Tanaka, M. Ueno, J. Yodoi, Antioxid. Redox Signal. 4 (2002) 405–414.
[39] S. Arora, J. Jain, J.M. Rajwade, K.M. Paknikar, Toxicol. Lett. 179 (2008) 93–100.
[40] R. Foldbjerg, P. Olesen, M. Hougaard, D.A. Dang, H.J. Hoffmann, H. Autrup, Toxicol. Lett. 190 (2009) 156–162.
[41] S. Park, Y.K. Lee, M. Jung, K.H. Kim, N. Chung, E.K. Ahn, Inhal. Toxicol. 19 (2007) 59–65.
[42] X.B. Wang, H.Y. Gao, B.L. Hou, J. Huang, R.G. Xi, L.J. Wu, Arch. Pharm. Res. 30 (2007) 653–665.
[43] X. Chen, C. Deng, S. Tang, M. Zhang, Biol. Pharm. Bull. 30 (2007) 128–132.
[44] R. Rajagopalan, S.K. Ranjan, C.K. Nair, Mutat. Res. 536 (2003) 15–25.
[45] M. Premanathan, K. Karthikeyan, K. Jeyasubramanian, G. Manivannan, Nanomed.: Nanotechnol. Biol. Med. 7 (2011) 184–192.
[46] G. Huichen, H. Qian, N.M. Idris, Y. Zhang, Nanomed.: Nanotechnol. Biol. Med. 6 (2010) 486–495.
[47] Z.M. Markovic, L.M. Harhaji-Trajkovic, B.M. Todorovic-Markovic, D.P. Kepić, K.M. Arsikin, S.P. Jovanović, A.C. Pantovic, M.D. Dramićanin, V.S. Trajkovic, Biomaterials 32 (2011) 1121–1129.
[48] D.L. Wiggins, C.O. Granai, M.M. Steinhoff, P. Calabresi, Gynecol. Oncol. 56 (1995) 353–356.
[49] Z.N. Oltavi, C.L. Milliman, S.J. Korsmeyer, Cell 741 (1993) 609–619.
[50] E. Yang, J. Zha, J. Jockel, L.G. Boise, C.B. Thompson, S.J. Korsmeyer, Cell 80 (1995) 285–291.
[51] D.R. Green, J.C. Reed, Science 281 (1998) 1309–1312.
[52] G. Kroemer, N. Zamzami, S.A. Susin, Immunol. Today 8 (1997) 44–51.
[53] M.T. Lin, M.F. Beal, Nature 443 (2006) 787–795.